Article

TRANSPARENT PROCESS

THE EMBO JOURNAL

Histone H4K20 tri-methylation at late-firing origins ensures timely heterochromatin replication

Julien Brustel[1,2,†], Nina Kirstein[3,†], Fanny Izard[1,2,†], Charlotte Grimaud[1,2], Paulina Prorok[4], Christelle Cayrou[4], Gunnar Schotta[5], Alhassan F Abdelsamie[3], Jérôme Déjardin[4], Marcel Méchali[4], Giuseppe Baldacci[6], Claude Sardet[1,2], Jean-Charles Cadoret[6,*,‡], Aloys Schepers[3,‡,§,**] & Eric Julien[1,2,‡,***]

Abstract

Among other targets, the protein lysine methyltransferase PR-Set7 induces histone H4 lysine 20 monomethylation (H4K20me1), which is the substrate for further methylation by the Suv4-20h methyltransferase. Although these enzymes have been implicated in control of replication origins, the specific contribution of H4K20 methylation to DNA replication remains unclear. Here, we show that H4K20 mutation in mammalian cells, unlike in *Drosophila*, partially impairs S-phase progression and protects from DNA re-replication induced by stabilization of PR-Set7. Using Epstein–Barr virus-derived episomes, we further demonstrate that conversion of H4K20me1 to higher H4K20me2/3 states by Suv4-20h is not sufficient to define an efficient origin *per se*, but rather serves as an enhancer for MCM2-7 helicase loading and replication activation at defined origins. Consistent with this, we find that Suv4-20h-mediated H4K20 tri-methylation (H4K20me3) is required to sustain the licensing and activity of a subset of ORCA/LRWD1-associated origins, which ensure proper replication timing of late-replicating heterochromatin domains. Altogether, these results reveal Suv4-20h-mediated H4K20 tri-methylation as a critical determinant in the selection of active replication initiation sites in heterochromatin regions of mammalian genomes.

Keywords DNA replication origins; heterochromatin; histone H4K20 methylation

Subject Categories Chromatin, Epigenetics, Genomics & Functional Genomics; DNA Replication, Repair & Recombination

DOI 10.15252/embj.201796541 | Received 16 January 2017 | Revised 19 June 2017 | Accepted 7 July 2017 | Published online 4 August 2017

The EMBO Journal (2017) 36: 2726–2741

Introduction

Eukaryotic DNA replication is initiated at thousands of chromosomal sites, known as replication origins, which are scattered along the genome and activated in a well-defined order during S-phase (Rhind & Gilbert, 2013; Renard-Guillet *et al*, 2014). To ensure that replication origins are activated only once per cell cycle, the initiation of replication is separated into three tightly regulated steps (Remus & Diffley, 2009; Ding & MacAlpine, 2011; Leonard & Méchali, 2013). First, origins are selected by the binding of the hexameric origin recognition complex (ORC), as cells exit mitosis. In a second step termed "replication licensing", ORC serves as a scaffold for the subsequent association of CDC6 and CDT1, which together coordinate the loading of the MCM2-7 complex on chromatin to form the pre-replication complex (pre-RC) (Siddiqui *et al*, 2013). Finally, in S-phase, CDK and DDK kinases trigger pre-RC activation, resulting in the association of additional components and establishment of active replication forks (Bell & Botchan, 2013). Once origins have fired, the recruitment of pre-RC components on chromatin is inhibited until the onset of the following mitosis (Arias & Walter, 2007). Importantly, to provide a backup system when cells undergo replication stress, a large excess of origins is licensed during G1-phase and only a fraction of them are transformed in active replication initiation sites during S-phase (Blow *et al*, 2011). To date, the mechanisms that dictate whether an origin will be active or not in unperturbed S-phase are unclear.

Although metazoan replication origins tend to be enriched in GC-rich sequences and G4 quadruplex structures, they do not share a clear consensus sequence (Besnard *et al*, 2012; Fragkos *et al*, 2015; Prioleau & MacAlpine, 2016). Chromatin features, such as nucleosome positioning and histone modifications, are also involved in the selection of replication initiation sites (Smith and Aladjem,

1 Institut de Recherche en Cancérologie de Montpellier (IRCM), INSERM U1194, Institut Régional du Cancer (ICM), Montpellier, France
2 University of Montpellier, Montpellier, France
3 Research Unit Gene Vectors, Helmholtz Zentrum München, Munich, Germany
4 Institute of Human Genetics (IGH), CNRS, Montpellier, France
5 Biomedical Center Munich, Planegg-Martinsried, Germany
6 Institut Jacques Monod, UMR7592, CNRS and University Paris-Diderot, Paris, France
*Corresponding author. Tel: +33 1 57 27 80 74; E-mail: jean-charles.cadoret@ijm.fr
**Corresponding author. Tel: +49 89 31871509; E-mail: schepers@helmholtz-muenchen.de
***Corresponding author. Tel: +33 4 67 61 45 14; E-mail: eric.julien@inserm.fr
†These authors contributed equally to this work as first authors
‡These authors contributed equally to this work as senior authors
§Present address: Helmholtz Zentrum München, Institute for Diabetes and Obesity, Monoclonal Antibody Facility, Neuherberg, Germany

2014). Hence, origin activation follows a spatiotemporal program that is highly connected to the regulation of chromatin states, with origins in transcriptionally active chromatin firing earlier than those in repressed chromatin (McGuffee *et al*, 2013; Pope & Gilbert, 2013; Pope *et al*, 2014; Fragkos *et al*, 2015). Typically, early-firing origins are characterized by their proximity to a combination of activating chromatin marks, including acetylation of histone H3 and H4 tails and methylation at lysines (K) 4 and 79 of histone H3 (Picard *et al*, 2014; Cayrou *et al*, 2015; Smith *et al*, 2016). In contrast, little is known about chromatin modifications that control the formation and activity of late origins in heterochromatin regions.

Lysine 20 of histone H4 (H4K20) is the major methylated residue on the H4 tail that can exist as mono (H4K20me1)-, di (H4K20me2)-, or tri-methylation (H4K20me3) (Brustel *et al*, 2011; Jørgensen *et al*, 2013). While H4K20me2 is the predominant H4K20 methyl state found in 80% of total histone H4, H4K20me1 and H4K20me3 are less abundant and typically enriched in transcriptionally active and silent chromatin, respectively (Beck *et al*, 2012a). Recently, biochemical analysis performed with histone peptides revealed that H4K20me2 and H4K20me3 might serve as binding sites for mammalian ORC1 and its cofactors (Oda *et al*, 2010; Vermeulen *et al*, 2010; Beck *et al*, 2012b; Kuo *et al*, 2012), suggesting a potential role of these two histone marks in replication origin selection and activity. Consistent with this hypothesis, artificial recruitment of the H4K20me1 methyltransferase PR-Set7 (also known as SET8, SETD8, and KMT5A) at a specific locus can induce the recruitment of several ORC components in a manner depending on the presence of Suv4-20h1/h2 (also known as KMT5B and KMT5C), the enzymes that catalyze H4K20me2/3 from H4K20me1 (Schotta *et al*, 2008; Beck *et al*, 2012b). In addition, PR-Set7 is targeted for proteasome degradation during S-phase by the PCNA-CRL4^{cdt2} ubiquitin complex and failure to degrade PR-Set7 triggers DNA re-replication in Suv4-20h1-expressing cells (Tardat *et al*, 2010; Beck *et al*, 2012b). However, it remains unclear whether these enzymes have a broad role in the regulation of DNA replication origins or restrained to specific genomic regions. Furthermore, several puzzles remain including the fact that loss of Suv4-20h and H4K20me2/3 only leads to a partial reduction in cell growth during mouse development (Schotta *et al*, 2008). Likewise, H4K20 methylation is not essential for DNA replication initiation in *Drosophila* cells (McKay *et al*, 2015; Li *et al*, 2016) and H4K20 enzymes have also non-histone substrates (Takawa *et al*, 2012), which also question on the role, if any, of H4K20 methylation in the control of DNA replication origins.

In order to clarify these issues, we have investigated further the functions of H4K20 methylation and the associated H4K20 enzymes in the regulation of DNA replication. By expressing a histone H4 mutant unable to undergo methylation on lysine 20, we first provide evidence that unlike *Drosophila*, H4K20 methylation states are mandatory for proper DNA replication and contribute to DNA re-replication induced by PR-Set7 stabilization in mammalian cells. Although facilitating ORC recruitment on chromatin, we show that the conversion of H4K20me1 to higher H4K20me states is not sufficient to define an efficient origin *per se* but rather serves as an enhancer for MCM2-7 loading and replication activation at defined origins. In line with this, we reveal that Suv4-20h-mediated H4K20me3 stimulates the binding of ORCA-associated protein LRWD1/ORCA and pre-RC complex at a subset of late-firing origins, which is essential for the timely replication of heterochromatin during late S-phase.

Results

H4K20 methylation is critical for S-phase progression and PR-Set7 replication licensing functions

As shown in human U2OS cells (Appendix Fig S1), loss of mammalian PR-Set7 results in improper S-phase progression, which is in part attributed to defects in replication origin activity (Jørgensen *et al*, 2007; Tardat *et al*, 2007). To provide evidence that this S-phase phenotype is directly caused by a decrease in the levels of H4K20 methylation rather than defects in the methylation of other PR-Set7 targets, we examined the cell cycle of human U2OS cells transduced with a high titer of retroviral vectors encoding a FLAG-tagged histone H4^{K20A} mutant carrying a lysine to alanine substitution at position 20 (K20A). Cells transduced with a virus encoding a FLAG-tagged wild-type histone H4^{WT} were used as controls. As shown in Fig 1A and B, immunoblot analysis showed that both FLAG-tagged H4^{WT} and H4^{K20A} proteins were expressed at similar levels and were efficiently incorporated into chromatin 3 days after retroviral infection (Fig 1A, lanes 3 and 6), thereby leading to the replacement of half of the pool of the endogenous histone H4 (Fig 1B, top panel). Incorporation of FLAG-H4^{K20A} mutant into chromatin slightly increased PR-Set7 levels but led to a specific decrease in the global levels of the three methylated H4K20 states, with a stronger reduction for H4K20me1 and H4K20me3 (Fig 1B). Cell-cycle profiles of FLAG-H4^{WT} and FLAG-H4^{K20A} cells were then analyzed the same day by measuring the DNA content according to low (gates 1) and high (gates 2) levels of FLAG-H4 expression (Fig 1C; gates 1 and 2, respectively). We noticed that the amount of cells with the highest levels of H4^{K20A} (i.e., with the strongest decrease in H4K20me) was low compared to FLAG-H4^{WT}

Figure 1. H4K20 mutation affects S-phase progression and prevents DNA re-replication induced by PR-Set7 stabilization.

A Immunoblot analysis of histone H4 and FLAG-tagged histone H4 protein levels in FLAG-H4^{WT} and FLAG-H4^{K20A} U2OS cells and subjected to biochemical fractionation: Cytosolic (S1) and nuclear (S2) are soluble supernatants and P3 is the chromatin-enriched fraction. MEK1 was used as a control of soluble components and HCF-1 protein was used for control of chromatin fraction.

B Immunoblot analysis of PR-Set7 and the levels of acetylation and methylation of endogenous H4 and FLAG-tagged H4 in FLAG-H4^{WT} and FLAG-H4^{K20A} U2OS cells.

C FACS analysis of DNA content and FLAG signal in FLAG-H4^{WT} or FLAG-H4^{K20A} cells. DNA content was analyzed according to the low (gate 1) and high (gate 2) levels of FLAG-tagged histone H4 proteins.

D FACS analysis of DNA content in cells expressing similar levels (gate 1) of FLAG-tagged histone H4^{WT} and H4^{K20A} upon expression of the PR-Set7^{PIPmut} and PR-Set7$^{PIPmut+SETmut}$ mutants. Quantitation of re-replicating parental (No FLAG), FLAG-H4^{WT}, and H4^{K20A} cells upon PR-Set7^{PIPmut} expression. Data are means ± SD, $n = 3$. (*) Statistical significance with $P < 0.05$ (*t*-test).

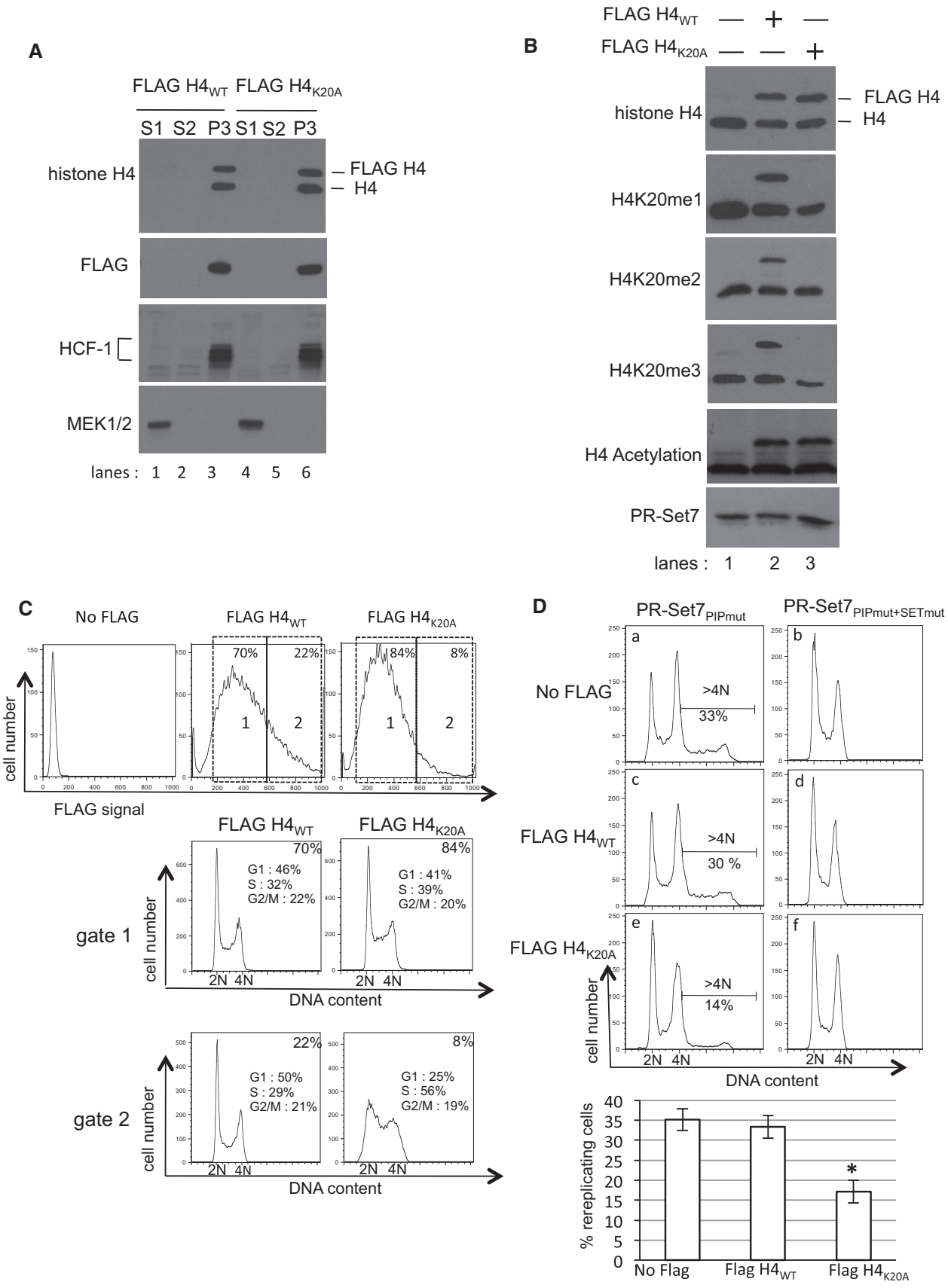

Figure 1.

cells (Fig 1C, upper panels, compare gates 1 and 2), suggesting that the H4K20A mutation is relatively toxic. Conspicuously, whereas cells with low levels of $H4^{K20A}$ displayed a cell-cycle profile similar to FLAG-$H4^{WT}$ cells (Fig 1C, gates 1), cells expressing high levels of FLAG-$H4^{K20A}$ accumulate in S-phase, suggesting that they fail to complete DNA replication as previously described in PR-Set7-depleted cells (Tardat *et al*, 2007; Appendix Fig S1).

Our results suggest that appropriate H4K20 methylation levels may be required for PR-Set7 functions in the licensing of replication origins. To verify this, we measured by FACS the levels of re-replication induced by the proteolytic-resistant PR-$Set7^{PIPmut}$ mutant in cell populations expressing similar and non-deleterious levels of FLAG-tagged $H4^{WT}$ or FLAG-tagged $H4^{K20A}$, 3 days before infection with retrovirus encoding PR-$Set7^{PIPmut}$ mutant (Fig 1C, gate 1). PR-$Set7^{PIPmut}$ contains mutations in the PCNA binding domain that inhibit $CRL4^{cdt2}$-mediated degradation and induce PR-Set7 stabilization (Tardat *et al*, 2010; Beck *et al*, 2012b). The resulting re-replication phenotype is caused by repeated PR-Set7-induced replication origin licensing (Tardat *et al*, 2010), which can be observed by the appearance of cells with DNA content greater than 4N, 2 days after PR-$Set7^{PIPmut}$ expression (Fig 1D, panel a). As shown in Fig 1D, expression of the PR-$Set7^{PIPmut}$, but not of the catalytic inactive PR-$Set7^{PIPmut+SETmut}$ mutant, caused the appearance of ~30% of re-replicated cells in both parental and FLAG-tagged $H4^{WT}$ cells (Fig 1D, compare panels a–d). In contrast, the level of re-replication upon PR-$Set7^{PIPmut}$ expression was greatly reduced in FLAG-tagged $H4^{K20A}$ cells (Fig 1D, panels e–f) correlating with the reduced amount of H4K20 residues in these cells. These results provide the evidence that H4K20 methylation is indeed a critical downstream effector of PR-Set7 replication licensing functions.

H4K20 methylation is an enhancer of origin efficiency

K20 methylation enhances histone H4 interaction with ORC *in vitro* (Beck *et al*, 2012b), suggesting that this histone mark might be sufficient to induce DNA replication at specific loci *in vivo*. To test this possibility, we examined the impact of H4K20 methylation on the replication of Epstein–Barr virus-derived (EBV) episomes from origin DNA sequences that involve cellular pre-RC complex for licensing. As illustrated in Fig 2A, the replication and stability of EBV episomes require the binding of the EBV-encoded protein EBNA1 to two DNA elements: (i) the family of repeats (FR) element that ensures the segregation and stability of episomes during cell division and (ii) the dyad symmetry (DS) element that serves as replication origin in human cells by co-recruiting ORC to this DNA sequence (Hammerschmidt & Sugden, 2013). To assess whether PR-Set7-induced H4K20 methylation on chromatin induces origin activity by its own, a GAL4-binding UAS sequence was introduced into a DS-deleted EBV plasmid named FR-UAS, which is incompetent for replication but not for EBN1A-mediated segregation. We then examined the rescue of the replication competence of this plasmid in HEK293 cells stably expressing EBNA1 and either GAL4 DNA-binding domain (GAL4), the wild-type GAL4-PR-$Set7^{WT}$, or the methylase-deficient GAL4-PR-$Set7^{SETmut}$ fusion proteins (Fig EV1A). HEK293 cell line was chosen because it is suitable for transfection and EBV episome replication (Gerhardt *et al*, 2006). As observed previously (Beck *et al*, 2012b), quantitative chromatin immunoprecipitation (ChIP-qPCR) showed that GAL4-PR-Set7 binding at the UAS site, but not of the GAL4 or GAL4-PR-$Set7^{SETmut}$ proteins, led to a local increase in H4K20me1 followed by its conversion to higher H4K20me states, as indicated by the appearance of high H4K20me3 enrichment at this locus (Fig EV1B). To measure episome replication efficiency, low molecular weight DNA was harvested 6 days after plasmid transfection and the number of replicated episomes was quantified by bacterial transformation after DpnI digestion to eliminate the bacterial-derived plasmids initially transfected into GAL4 cell lines. The results are shown in Fig 2B. As controls, similar experiments were performed with the wild-type FR-DS plasmid and the FR-ORI^{RDH} plasmid (Fig 2A), which contains the 300-bp ORC-binding DNA fragment of the human replication origin (ORI^{RDH}) of the *RDH* gene instead of the DS element (Gerhardt *et al*, 2006). The results are shown in Fig 2B. Compared to the FR-DS plasmid, the FR-ORI^{RDH} plasmid displayed a low replication competence in all cell lines (Fig 2B), which is representative of the low efficiency of short mammalian origin DNA sequences to define an origin by their own (Gerhardt *et al*, 2006). We noticed that the replication of the FR-UAS plasmid was almost undetectable in GAL4 and GAL4-PR-$Set7^{SETmut}$ cells but not in GAL4-PR-Set7-expressing cells, where this plasmid exhibited a low replication similar to that of the FR-ORI^{RDH} plasmid (Fig 2B). These results indicate that a local increase in H4K20 methylation, as observed with mammalian DNA sequences, is not sufficient to define a fully competent origin of replication.

Since origin efficiency might depend on the presence of multiple origin determinants (Méchali *et al*, 2013; Valton *et al*, 2014), we next examined the effect of inducing H4K20 methylation in the vicinity of the ORI^{RDH} origin. For this, we created the FR-UAS-ORI^{RDH} plasmid (Fig 2A) and tested the replication competence of this plasmid as described above. As shown in Fig 2D, the ORI^{RDH} efficiency in FR-UAS-ORI^{RDH} plasmid was fourfold increased in GAL4-PR-Set7 cells, whereas it remained unchanged in GAL4 and GAL4-PRSet7^{SETmut} cells (Fig 2C). ChIP-qPCR analysis showed that this stimulation of ORI^{RDH} activity GAL4-PR-Set7 cells was associated with an accumulation of H4K20me1/me3 and a higher efficiency of MCM2-7 loading, as measured by the significant increase in the levels of MCM3 at the UAS and ORI^{RDH} sequences in FR-UAS-ORI^{RDH} plasmid (Fig 2D). Importantly, the same enhancer

Figure 2. H4K20 methylation enhances origin formation and activity.

A Schematic representation of EBN1A protein and studied EBV-derived plasmids with the relative position of DNA fragments amplified during ChIP-qPCR experiments.

B Quantitation of replicating FR-DS, FR-UAS, and FR-ORI^{RDH} plasmids in cells expressing EBNA1 and either GAL4, GAL4-PR-Set7, or GAL4-PR-$Set7^{SETmut}$. Data are means ± SEM (n = 4) with control FR-DS plasmid arbitrarily set as one in every cell line (gray bars).

C Quantitation of replicating FR-UAS-ORI^{RDH} and FR-ORI^{RDH} in the same cell lines as above. Data are means ± SEM (n = 4) relative to FR-ORI^{RDH} (black bars). (*) Statistical significance (paired two-tailed t-test) with $P < 0.05$.

D ChIP-qPCR analysis at ORI^{RDH}, UAS, and FR sequences in different GAL4 cell lines transfected with FR-ORI^{RDH} or FR-UAS-ORI^{RDH} plasmids using antibodies as indicated. Data are means ± SEM (n = 4) as fold enrichment of the each antibody relative to isotype IgG control. (*) Statistical significance (paired two-tailed t-test) with $P < 0.05$.

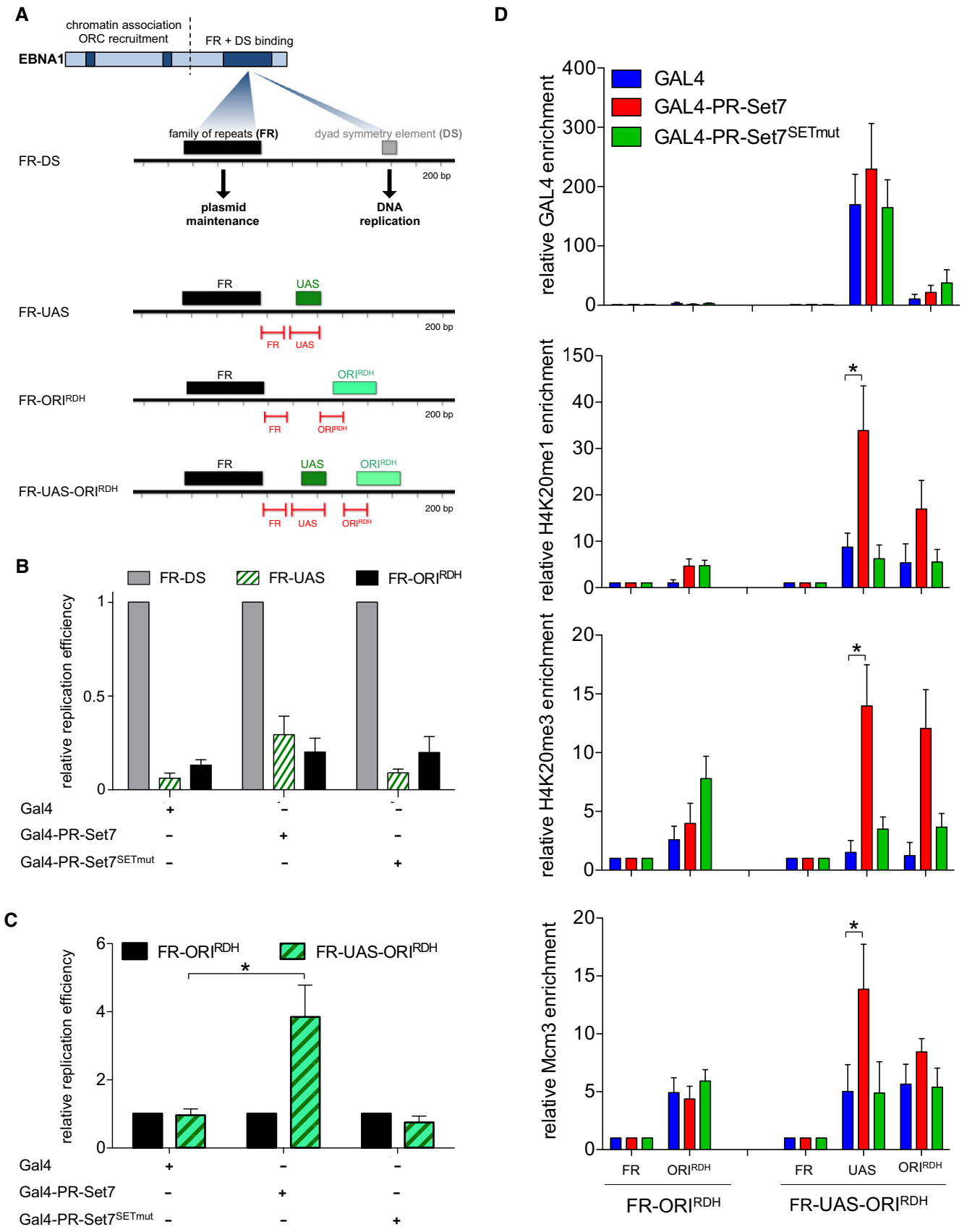

Figure 2.

effect on MCM2-7 loading and origin activity was also observed for the viral origin sequence oriP in a FR-UAS-DS plasmid transfected in GAL4-PR-Set7-expressing cells (Fig EV1B and C), confirming the ability of PR-Set7-induced H4K20 methylation to stimulate replication initiation at defined origins. Taken together, these results show that PR-Set7-induced H4K20 methylation is likely not sufficient to promote efficient origin function but rather serves to strengthen the activity of defined origins by enhancing the recruitment and/or stability of pre-RC complexes at these origins.

PR-Set7-mediated stimulation of origin activity depends on the further methylation of H4K20me1 by Suv4-20h1/h2

Since the ORC shows a higher affinity for H4K20me2/3 than for H4K20me1 *in vitro* (Oda *et al*, 2010; Vermeulen *et al*, 2010; Kuo *et al*, 2012), we asked whether the stimulatory effect of H4K20 methylation on origin activity depends on the switch from H4K20me1 to higher H4K20me states induced by Suv4-20h1/h2 methyltransferases. To address this question *in vivo*, we repeated the replication assay with FR-ORI^{RDH} and FR-UAS-ORI^{RDH} plasmids in GAL4-PR-Set7 cells in the presence of A-196, a chemical inhibitor of Suv4-20h1/h2. Immunoblot analysis of whole-cell extracts confirmed the specificity of the A-196 treatment, which led to a strong reduction in the levels of H4K20me2/3 and the subsequent increase in H4K20me1 without an impact on the levels of histone H3 tri-methylation at lysines 4, 9, and 27 (Appendix Fig S2). Consistent with these results, ChIP-qPCR analysis showed that H4K20me1, but not H4K20me3, was highly enriched at the UAS and ORI^{RDH} sequences in GAL4-PR-Set7-expressing cells treated with A-196 (Fig 3A). In this experimental context, the FR-UAS-ORI^{RDH} and FR-ORI^{RDH} plasmids displayed a similar replication activity without any significant difference in the levels of MCM3 loading at the ORI^{RDH} origin (Fig 3B and C). These results confirm that PR-Set7-mediated H4K20me1 is only a prerequisite for replication origin stimulation (Beck *et al*, 2012b), which depends on additional methylation of H4K20me1 by Suv4-20h enzymes.

Loss of Suv4-20h activity on H4K20me1 specifically impairs heterochromatin replication timing

We next sought to determine whether the ability of Suv4-20h and higher H4K20 methylation states to enhance replication origin activity plays an essential role in the replication of all the genome or only at specific chromatin regions. To address this question, we examined at genome-wide levels the spatiotemporal replication program of mouse embryonic fibroblast (MEF$^{364.2}$) line derived from *Suv4-20h2*$^{-/-}$, *Suv4-20h1*$^{-/flox}$, Cre-ER embryos and in which the remaining knocked-in floxed *SUV4-20H1* gene can be deleted by addition of 4-hydroxytamoxifen (4OHT). Four days after 4OHT treatment, immunoblot analyses showed a complete and irreversible

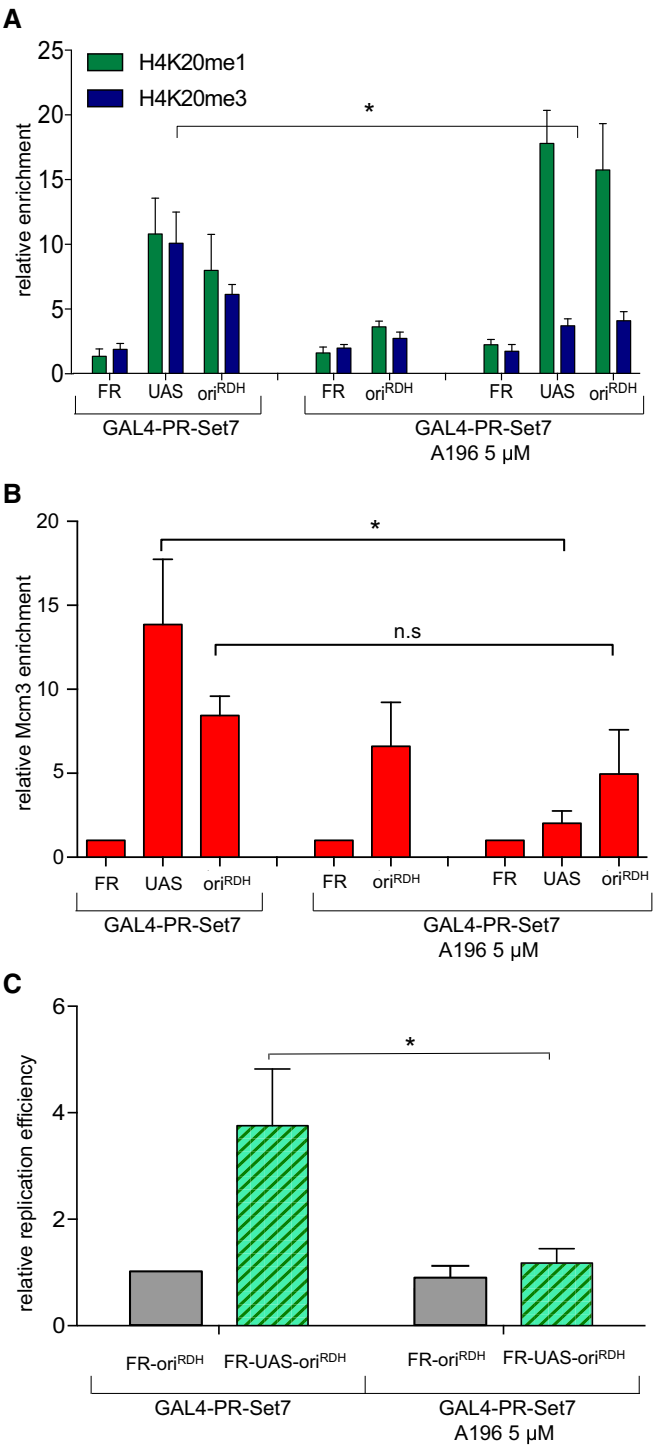

Figure 3. PR-Set7 improves origin activity through Suv4-20h activity on H4K20me1.

A ChIP-qPCR analysis of H4K20me1 and H4K20me3 levels at ORI^{RDH}, UAS, and FR in the HEK293 EBNA1^{+} Gal4-PR-Set7-expressing cell line in the absence (left panel) and presence of the Suv4-20h inhibitor A196 (right panels). Data are means ± SEM (n = 4).

B ChIP-qPCR analysis of MCM3 levels at ORI^{RDH}, UAS, and FR in EBNA1/Gal4-PR-Set7-expressing cell lines in the absence (left panel) and presence of A196 (right panel). Data are means ± SEM (n = 4).

C Quantitation of replicating FR-ORI^{RDH} (black) and FR-UAS-ORI^{RDH} (striped) plasmids in EBNA1/GAL4-PR-Set7-expressing cells in the presence and absence of A196. The replication efficiency is relative to ORI^{RDH} in untreated cells. Data are means ± SEM (n = 4).

Data information: Significance was determined employing an unpaired two-tailed t-test. *$P < 0.05$.

disappearance of H4K20me2 and H4K20me3 followed by a concomitant accumulation of H4K20me1 in MEFs$^{364.2}$ (Fig 4A, left panels). At this time, untreated and 4OHT cells were pulse-labeled with BrdU and sorted into early and late S-phase fractions by flow cytometry. Nascent BrdU-substituted DNA of each fraction was then isolated and labeled with fluorescence dyes before hybridization on microarrays covering the mouse genome, at the exception of centromeric and telomeric regions, with one probe every 13 kb. The replication timing of these cells was determined using the Agilent CGH algorithm that generates a log ratio value corresponding to early-replicating regions when the log ratio is positive and to late-replicating regions when the log ratio is negative. As illustrated in Fig 4A for a fragment of chromosome 11 (right panel), the loss of Suv4-20h in 4OHT-treated MEFs$^{364.2}$ specifically delays the replication of some mid- and late-replicating chromatin domains, whereas the replication of early domains remained largely unaffected. Consistent with these results, 4OHT-treated MEFs$^{364.2}$ displayed a lower proliferation rate and tended to accumulate in late S-phase as shown by FACS analysis (Fig EV2A and B). Furthermore, replication-timing delays of the same chromatin regions were also observed in fibroblast lines derived from *Suv4-20h1/2* knockout embryos (Fig EV2C), thereby indicating that the disrupted replication pattern upon loss of Suv4-20h was highly reproducible and cell line independent. To verify that the replication-timing alterations observed in 4OHT-treated MEFs$^{364.2}$ are indeed triggered by the loss of H4K20me2/3 states, we generated as described above the replication-timing profile of untreated MEF$^{364.2}$ expressing similar levels of FLAG-tagged histone H4^{WT} or H4^{K20A}. As shown in Fig 4B, expression of histone H4^{K20A} led to a decrease in the levels of three H4K20 methylation states, which was followed by the same replication-timing alterations than those observed in 4OHT-treated MEFs$^{364.2}$ (see arrows in Fig 4A and B). In addition, we noticed that both histone H4^{K20A}- and H4^{WT}-expressing MEFs$^{364.2}$ displayed some replication-timing changes in early-replicating domains compared to untreated cells, which might be caused by the artificial expression of FLAG-tagged histone H4 proteins in these cells (compare Fig 4A and B, right panels). Conspicuously, although H4^{K20A} expression caused only a partial decrease in H4K20me2/3 levels compared to the loss of Suv4-20h, we found that 54% of replication-timing alterations in 4OHT-treated MEFs$^{364.2}$ were also detected in H4^{K20A}-expressing MEFs$^{364.2}$, demonstrating that these replication defects are indeed caused by the loss of Suv4-20h activity on H4K20me1.

Further analysis of replication-timing delays in 4OHT-treated MEFs$^{364.2}$ revealed that 80% of these delays occurred in late-replicating domains (Fig 4C). These domains correspond to large genomic regions with a median size of 2.2 megabases (Fig 4D). Quantification of these data shows that 114 distinct late-replication domains, which cover ~15% of the genome, displayed a significant replication-timing delay upon loss of Suv4-20h (P-value $< 1 \times 10^{-3}$). In mammalian cells, late-replication domains have been reported to be gene poor and often to coincide with heterochromatin regions (Rhind & Gilbert, 2013). In line with these results, the 114 altered replication domains exhibited the lowest gene density and coverage with activating chromatin mark H3K27 acetylation, but the highest coverage with the heterochromatin repressive mark H3K9me2 compared to stochastic or unmodified early/mid/late-replication domains in Suv4-20h-null cells (Fig 4E–G, statistical analysis in Appendix Table S1). Altogether, these results show that Suv4-20h activity on H4K20me1 is specifically required for the replication timing of late domains corresponding to heterochromatin regions.

High levels of H4K20me3 at origins are required for proper heterochromatin replication

Since H4K20me3 is a hallmark of heterochromatin (Schotta *et al*, 2004), we next examined by ChIP-qPCR whether H4K20me3 is particularly enriched at replication origins in late-replicating heterochromatin domains that were delayed in Suv4-20h-null cells. The results of four replication origins randomly selected in a delayed domain and of four origins in a non-delayed late domain of the chromosome 11 are shown in Fig 5. Moreover, the results of 10 additional origins in different delayed and non-delayed late domains are shown in Fig EV3A. The localization of all these origins was previously found by nascent DNA strand purification in MEF lines (Cayrou *et al*, 2011, 2015). Compared to a control origin in an early-replicating domain and a flanking negative sequence (NEG) close to ORI-1, the levels of H4K20me3 at origins in non-delayed late domains were generally weak or close to background levels in all cellular

Figure 4. Loss of Suv4-20h impairs the timing of late-replicating heterochromatin.

A Immunoblot analysis (left panel) of H4K20me1, H4K20me2, and H4K20me3 levels and replication-timing profile (right panel) of a 23-Mb fragment of chromosome 11 (cytogenetic coordinates qA31 to qB1.2) in MEFs$^{364.2}$ untreated or 4 days after 4-hydroxytamoxifen (4OHT) treatment. Arrows point to delayed domains in 4OHT-treated cells.

B Immunoblot analysis (left panel) of histone H4, H4K20me1, H4K20me2, and H4K20me3 levels and replication-timing profile (right panel) of the same fragment of chromosome 11 as above in MEFs$^{364.2}$ 5 days after transduction with retrovirus encoding histone H4^{WT} or H4^{K20A} mutant. Arrows point to delayed domains in H4^{K20A}-expressing cells.

C Box-plot showing the percentage of delayed replication domains in each timing categories in 4OHT-treated MEFs$^{364.2}$.

D Size distribution (megabase) of delayed domains in MEFs$^{364.2}$ treated with 4OHT.

E Box-plot showing gene coverage (percentage) in unaffected early, mid-, and late domains, in delayed domains, and in stochastic replication domains of 4OHT-treated MEFs$^{364.2}$.

F Box-plot showing H3K27ac coverage levels in unaffected early, mid-, and late domains, and in delayed domains, and in stochastic replication domains of 4OHT-treated MEFs$^{364.2}$.

G Box-plot showing H3K9me2 coverage levels in unaffected early, mid-, and late domains, in delayed domains, and in stochastic replication domains of 4OHT-treated MEFs$^{364.2}$.

Data information: (*) Statistical significance was detected when a Student's test (t-test) was performed with $P < 10^{-3}$ (see Appendix Table S1 for detailed statistical analysis). Inside the box-plot graphs, the thick line represents the median, the limit of the boxes corresponds to the 0.25 to 0.75 quartiles with whiskers extending to the maximum value of 1.5 times the interquartile range.

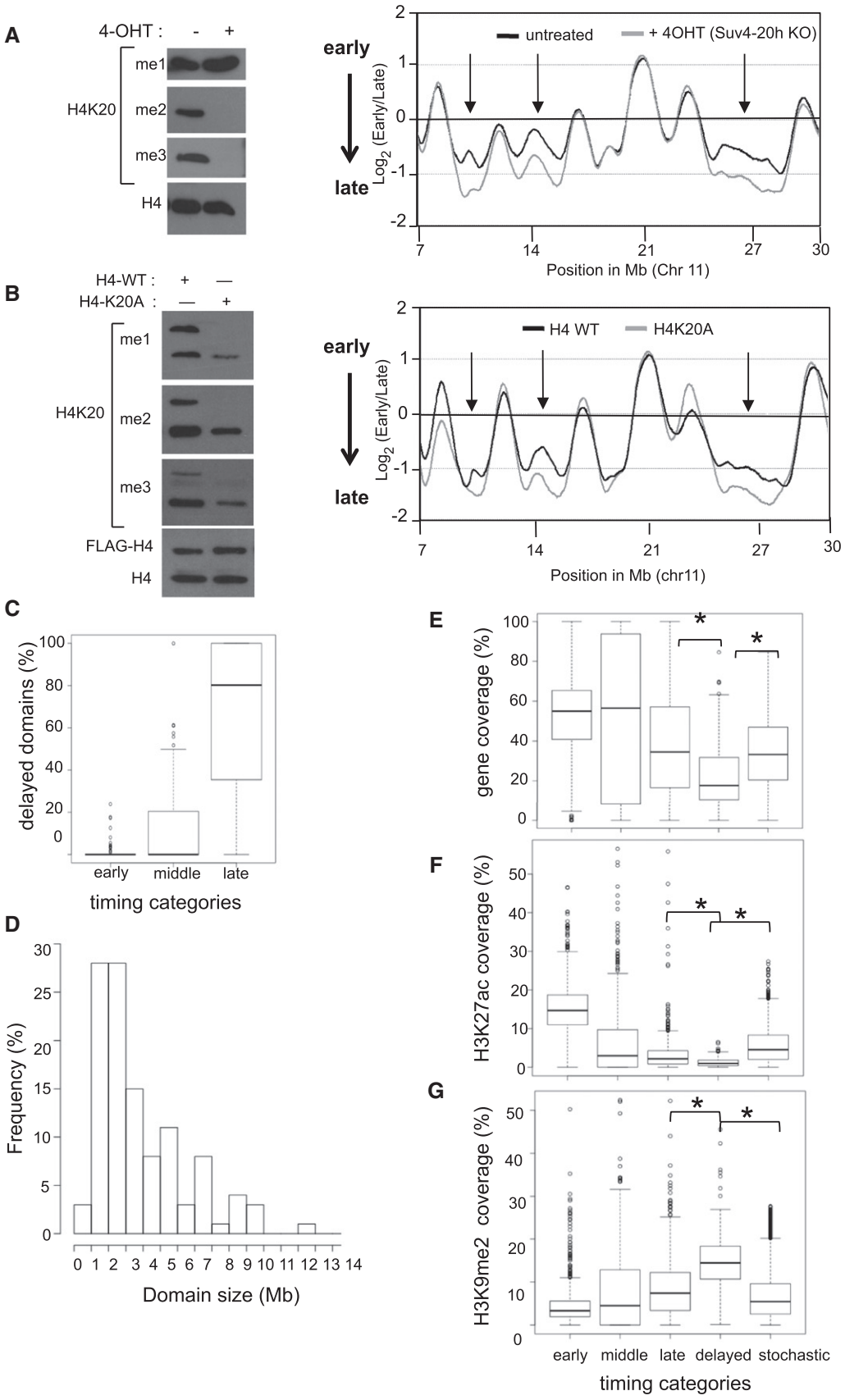

Figure 4.

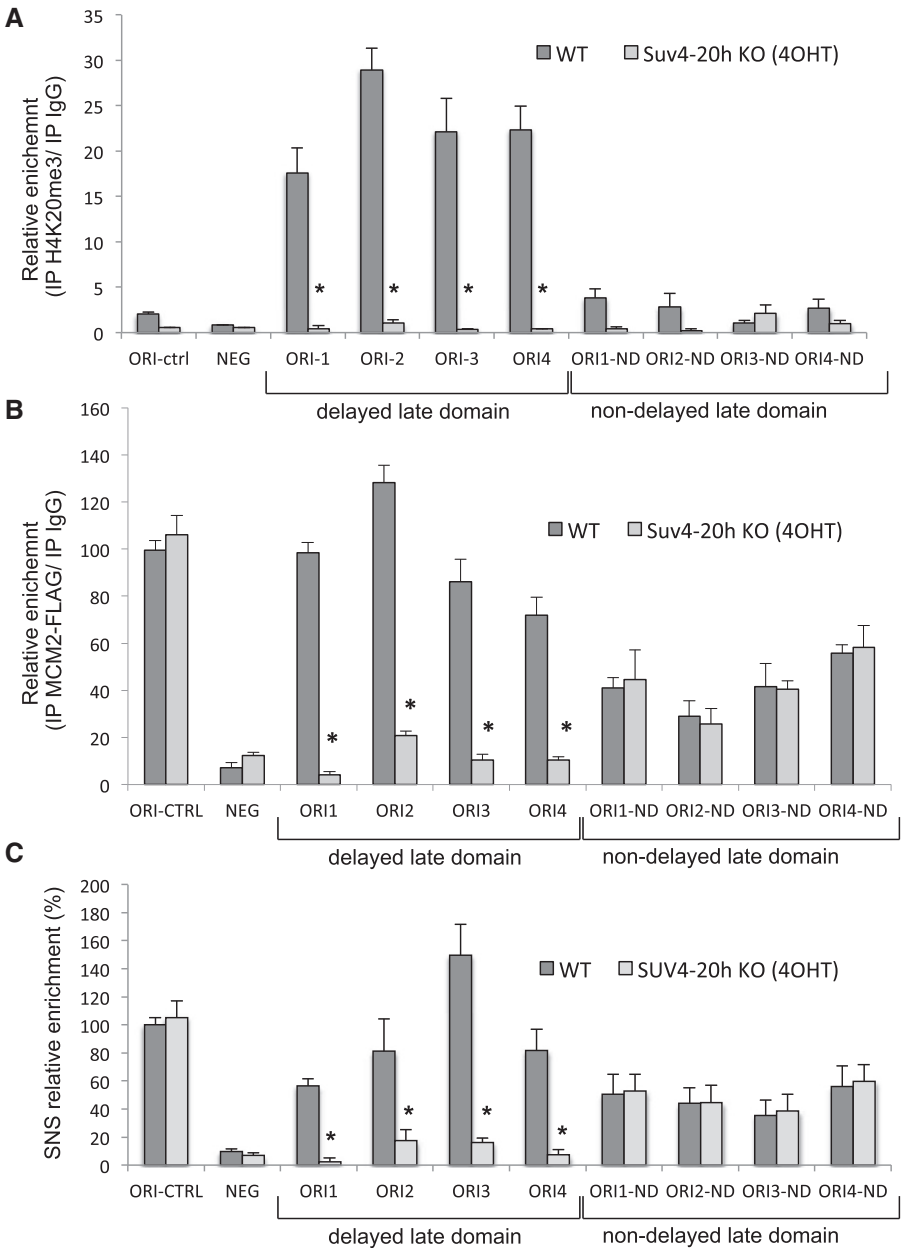

Figure 5. Suv4-20h-mediated H4K20me3 is required for the appropriate licensing and activity of a subset of origins in late-replicating heterochromatin.

A ChIP-qPCR analysis of H4K20me3 levels at the control early-firing MYC origin and at origins in delayed and non-delayed late domains of chromosome 11 in untreated and 4OHT-treated MEFs$^{364.2}$ using anti-H4K20me3 and an isotype non-relevant antisera (IgG) as control. NEG corresponds to a negative control region 5 kb downstream of ORI-1. Coordinates of studied ORIs are indicated in Appendix Table S2. Errors bars represent SD (n = 3).

B ChIP-qPCR analysis of MCM2 levels at the same origins as above in untreated and 4OHT-treated MEFs$^{364.2}$ stably expressing FLAG-tagged MCM2 and using anti-FLAG or IgG as ChIP control. Errors bars represent SD (n = 3).

C Quantitation of the relative SNS enrichment of the same origins as above origin in untreated and 4OHT-treated MEFs$^{364.2}$ and arbitrarily normalized with respect to the control origin. Data are means ± SD (n = 3).

Data information: (*) Statistical significance with $P < 0.001$ (unpaired t-test).

conditions, whereas a peak of H4K20me3 was detected at almost all origins in delayed late domains before but not after 4OHT treatment (Figs 5A and EV3A). Consistent with these results, H4K20me1 was found highly enriched instead of H4K20me3 at these origins in 4OHT-treated cells (Fig EV3B). Importantly, the decrease in H4K20me3 levels at origins in delayed late domains was also observed in H4^{K20A}-expressing MEF$^{364.2}$ (Fig EV4A), thereby suggesting that the replication-timing alterations upon loss of Suv4-20h-mediated H4K20 methylation principally occur in heterochromatin regions where origins are normally associated with high levels of H4K20me3.

To determine whether the lack of H4K20me3 has indeed an impact on the licensing and activity of these origins, wild-type as

well as $H4^{WT}$- and $H4^{K20A}$-expressing $MEFs^{364.2}$ were transduced with retroviral vectors encoding FLAG-tagged MCM2 or MCM5 and ChIP-qPCR experiments were performed with FLAG antibody to measure pre-RC formation at different origins. In parallel, we isolated and quantified by qPCR the levels of short nascent DNA strands at these origins (SNS), which is a direct measure of their efficiency (Valton *et al*, 2014). As shown in Figs 5B and C, and EV4B–D, all origins tested were normally associated with FLAG-tagged MCM5 and/or MCM2 proteins and displayed high SNS levels in untreated or $H4^{WT}$ cells. In contrast, whereas the loading of MCM proteins and the activity of origins in non-delayed late domains largely remained unaffected, the abrogation of H4K20me3 upon 4OHT treatment or its decrease in $H4^{K20A}$ cells coincided with the inability of H4K20me3-associated origins to recruit appropriate levels of MCM proteins and to efficiently initiate DNA synthesis (Figs 5B and C, and EV4B–D). These results show that high levels of H4K20me3 are critical for the full activity of an important subset of late-firing origins, thereby explaining the delay in heterochromatin replication observed in Suv4-20h and H4K20 methylation-depleted cells.

ORCA/LRWD1 binding to H4K20me3-associated late-firing origins is required for heterochromatin replication

Previous studies have shown that tri-methylated H4K20 peptides can directly interact *in vitro* with the WD40 domain of the ORCA-associated protein ORCA/LRWD1 (Beck *et al*, 2012b), which is suspected to play an important role in the replication and organization of heterochromatin by facilitating the recruitment of ORC (Wang *et al*, 2016). We therefore reasoned that H4K20me3 might ensure the proper replication timing of heterochromatin by inducing the recruitment of ORCA at specific late-firing origins. To test this hypothesis, FLAG-tagged ORCA was stably expressed in the different $MEFs^{364.2}$ lines and the ability of this protein to associate with origins in delayed and non-delayed late domains of the chromosome 11 was evaluated by ChIP-qPCR in Suv4-20h-null and $H4^{K20A}$-expressing cells. Whereas FLAG-tagged ORCA was found associated with all origins tested in untreated and $H4^{WT}$ cells, the abrogation of H4K20me3 upon Suv4-20h inactivation or $H4^{K20A}$ expression coincided with the inability of ORCA to associate specifically with the set of origins that are normally highly enriched in this methylation mark (Figs 6A and EV5). Consistent with the absence of ORCA binding to this specific subset of late-firing origins, which control the replication of ~15% of the mouse genome (Fig 4), the amount of chromatin-associated pool of ORCA was reduced of 40% in Suv4-20h-null cells compared to control cells (Fig 6B). Altogether, these results suggest that ORCA may associate with origins through multiple mechanisms and that the binding of ORCA to H4K20me3 is specifically required for its association with a subset of late-firing origins.

To determine whether the recruitment of ORCA to H4K20me3-enriched origins is necessary for the activity of these origins and the proper replication of associated late domains, we induced the silencing of ORCA by two independent shRNA (Fig 6C) and then examined the replication timing and activity of H4K20me3-associated origins in ORCA-depleted cells as described above. Although ORCA was not fully depleted (Fig 6C), the replication of mid- and late-replicating domains was delayed in shRNA ORCA-treated cells, while early-replicating domains remained unchanged or eventually slightly advanced (Fig 6D and Appendix Fig S3). Clearly, 64% of late-replicating domains delayed in Suv4-20h-null and $H4^{K20}$-expressing cells were also found significantly altered in ORCA-depleted cells, as shown for the same fragment of chromosome 11 in the three cellular conditions (compare Figs 4A and B, and 6D). In line with these results, we found that ORCA depletion impairs the levels of MCM loading and replication initiation at H4K20me3-associated origins (Fig 6E and F). Moreover, consistent with the ability of ORCA to interact with Suv4-20h (Giri & Prasanth, 2015), ORCA depletion also caused a significant reduction of H4K20me3 at these origins, thereby indicating a mutual dependence between the binding of ORCA and the accumulation of high levels of H4K20me3 at these sites (Fig 6G). Taken together, these results suggest a model where the timely replication of a large fraction of heterochromatin regions in mammalian cells depends on the concerted activities of PR-Set7 and Suv4-20h in order to generate H4K20me3-mediated ORCA binding at a subset of late-firing origins and thus to enhance the licensing and efficiency of these origins.

Discussion

This study provides new insights into the role of H4K20 methylation in the control of DNA replication in mammalian cells. First, we demonstrate that H4K20 methylation is a critical effector of PR-Set7

Figure 6. ORCA/LRWD1 binds to H4K20me3-associated origins and promotes the licensing and activity of these origins.

A ChIP-qPCR analysis of ORCA levels at the same origins as in Fig 5 in untreated and 4OHT-treated $MEFs^{364.2}$ stably expressing FLAG-tagged ORCA and using anti-FLAG or IgG as a control. NEG corresponds to a negative ORCA binding site. Errors bars represent SD (n = 3).

B Immunoblot analysis of HCF-1 and ORCA proteins in whole-cell extracts (inputs) and in chromatin-enriched fraction in untreated and 4OHT-treated $MEFs^{364.2}$. Chromatin-bound HCF-1 protein was used as control of chromatin purification. Quantitation of ORCA protein levels are indicated relative to HCF-1 and normalized with respect to the ORCA levels in untreated cells. (*) indicates a ORCA cleavage product in chromatin fraction after biochemical fractionation.

C Immunoblot analysis of ORCA and tubulin proteins in immortalized MEFs transduced with lentivirus encoding shRNA control or two independent shRNA ORCA. Quantitation of ORCA protein levels is indicated relative to tubulin and normalized with respect to the ORC levels in control cells.

D Replication-timing profile of the same 23-Mb chromosome fragment as in Fig 5A in MEFs treated with shRNA control or shRNA (2) ORCA. Arrows point to delayed late domains in ORCA-depleted cells.

E ChIP-qPCR analysis of MCM5 levels at the control early-firing MYC origin and H4K20me3-associated origins in control and ORCA-depleted MEFs expressing FLAG-tagged MCM5 and using anti-FLAG or IgG as ChIP control. Errors bars represent SD (n = 3).

F Quantitation of the relative SNS enrichment of the same origins as above. SNS enrichment was arbitrarily normalized with respect to the control origin. Errors bars represent SD (n = 2).

G ChIP-qPCR analysis of H4K20me3 levels at the same origins as above using anti-H4K20me3 and IgG as ChIP control. Errors bars represent SD (n = 3).

Data information: (*) Statistical significance (unpaired t-test) with $P < 0.05$ (for panels E–G) and $P < 0.005$ (for panel A).

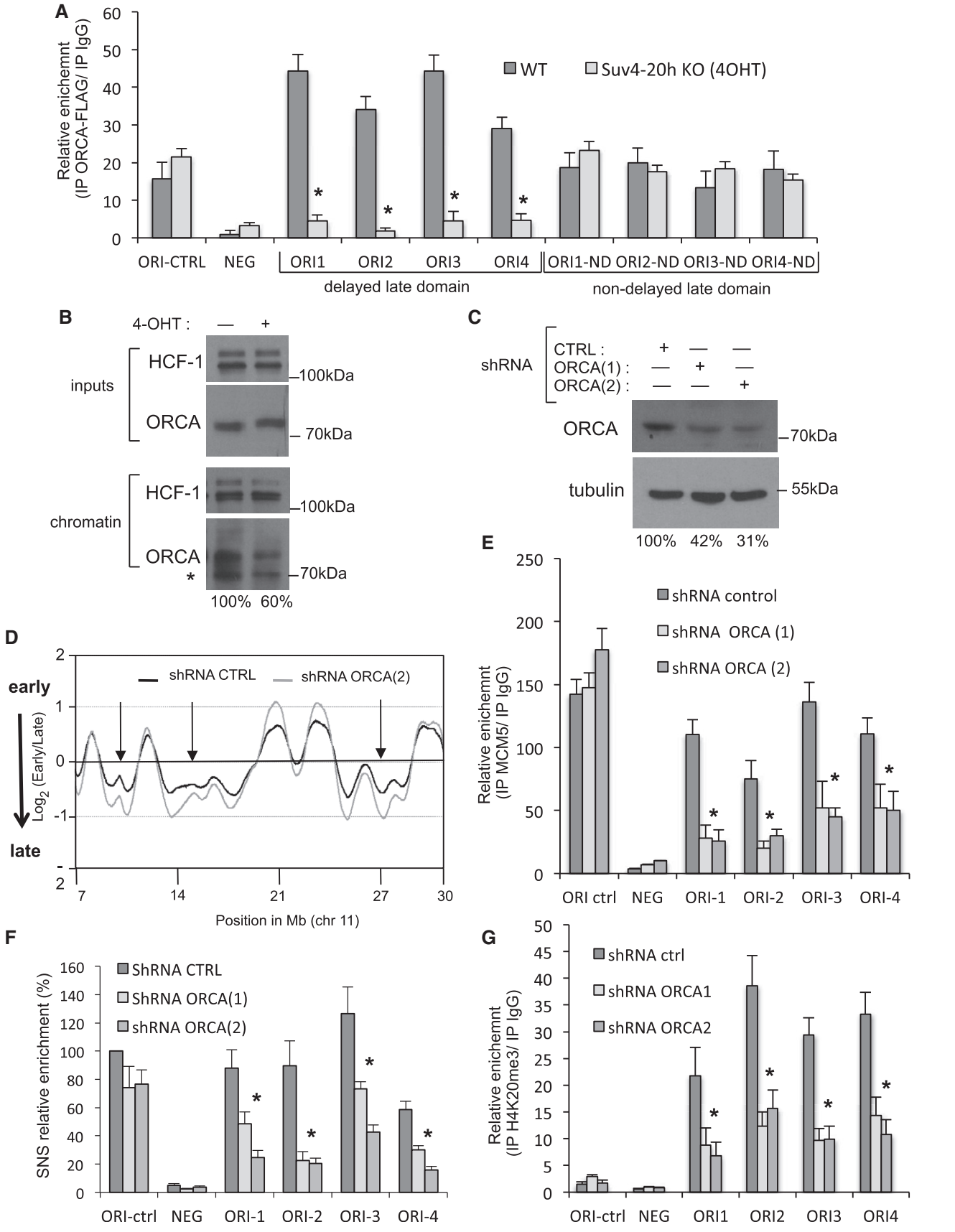

Figure 6.

replication licensing functions and appropriate levels of this methylation mark are important for faithful and timely progression through S-phase (Fig 1). Together with origin DNA sequences, we show that a local increase in PR-Set7-induced H4K20me1 followed by its conversion to higher H4K20me states by Suv4-20h is not sufficient to define a functional origin *per se* and rather serves to enhance replication origin activity by improving MCM2-7 loading (Figs 2 and 3). Moreover, we reveal that the loss of Suv4-20h and H4K20me methylation impair the licensing and activity of a subset of late-firing origins, which delay the replication of 15% of the genome mostly at the levels of heterochromatin domains (Figs 4 and 5). Finally, we show that the recruitment of ORCA and the associated pre-RC complex at these defined late-firing origins depends on Suv4-20h-mediated H4K20me3, which is therefore essential for proper heterochromatin replication (Figs 5 and 6). Altogether, these results place H4K20 methylation and the degree of this methylation, through the concerted activities of PR-Set7 and Suv4-20h, as a critical determinant in the selection of active replication initiation sites in heterochromatin regions of mammalian genomes.

Although previous studies have shown that the role of PR-Set7 in replication origin licensing is connected to Suv4-20h (Beck *et al*, 2012b), it still remained unclear whether H4K20 methylation was the effector of these enzymes in the control of DNA replication. Indeed, PR-Set7 and Suv4-20h are also known to interact with and target non-histone proteins important for DNA replication and flies harboring a histone H4 with a K20A substitution are viable, although sick, with no apparent DNA replication defects (McKay *et al*, 2015). By taking advantage that mammalian cells can rapidly adapt the levels of endogenous histone H4 in response to an ectopic histone H4 expression, we replaced a large fraction of the pool of histone H4 with histone H4K20A mutant and thus directly assessed the role of H4K20 methylation in mammalian cell-cycle progression. Although we cannot exclude non-histone substrates being also involved, our results demonstrate that H4K20 methylation is indeed required for PR-Set7 and Suv4-20h functions at replication origins in mammalian cells. Thus, the role of H4K20 methylation in replication origin activity is likely specific to mammals, which is corroborated by the absence of replication origin activation defects in *Drosophila Suv4-20h* mutant and in *Drosophila* Kc167 cells depleted for PR-Set7 (Sakaguchi *et al*, 2008; Li *et al*, 2016). H4K20 methylation is actually not the unique replication origin feature that may differ between *Drosophila* and mammalian models. Although enhanced DNA flexibility similarly marks *Drosophila* and mammalian replication origins, the sequence composition of these origins is remarkably different between these two organisms (Lombraña *et al*, 2013; Picard *et al*, 2014; Comoglio *et al*, 2015). Furthermore, *Drosophila* replication initiation sites are generally poor in nucleosomes (Liu *et al*, 2015), while a versatile nucleosome occupancy is often found at mammalian replication initiation sites (Cayrou *et al*, 2011; Lombraña *et al*, 2013). Thus, the role of H4K20 methylation in DNA replication could have emerged with a differential nucleosome contribution to origin specification and activity in mammals.

It is becoming increasingly evident that flexible combinations of genetic and epigenetic features are responsible for the recruitment of pre-RC complex and participate in the proper control of replication origin activation (Leonard & Méchali, 2013). Consistent with this idea, GC-rich DNA sequences contribute to origin specification but requires the presence of other elements to define a fully competent replication origin in mammalian cells (Valton *et al*, 2014). Similarly, using EBV-derived episomes, we showed that PR-Set7-induced H4K20me1 and its subsequent conversion to higher H4K20me states by Suv4-20h constitute a weak specificity factor for origin. Instead, our results suggest that Suv4-20h activity on H4K20me1 marks can enhance origin efficiency when this methylation activity is combined with genetic origin features (Figs 2 and 3). We also showed that Suv4-20h stimulates the activity of replication origins by increasing or stabilizing the levels of MCMs at origin DNA sequences. This is in agreement with previous studies showing that multiple MCMs can be loaded at origins and that this excess of MCM proteins increases origin efficiency (Bowers *et al*, 2004; Das *et al*, 2015).

How might Suv4-20h activity improve MCM2-7 helicase loading at specific loci? Since the BAH domain of ORC1 and the WD40 domain of ORCA display a high affinity for H4K20me2 and H4K20me3, respectively (Oda *et al*, 2010; Beck *et al*, 2012b; Kuo *et al*, 2012), one simple explanation is that the subsequent methylation of H4K20me1 by Suv4-20h at specific origins would enhance the affinity of ORC for these origins, resulting in a higher ORC occupancy or stability that in turn favors a more efficient MCM recruitment and higher origin efficiency. Interestingly, our replication-timing analysis of Suv4-20h-null and histone $H4^{K20A}$-expressing cells suggests that this enhancer function of H4K20 methylation marks on origin activity is likely specific to late-replicating origins in silent chromatin regions, which are naturally less favorable for MCM2-7 loading. It is somehow reminiscent of the differential ORC-origin binding mechanisms in *S. cerevisiae*, where the high affinity of ORC for specific DNA sequences is required for late-firing origins and heterochromatin formation (Palacios DeBeer *et al*, 2003; Hoggard *et al*, 2013). However, the mammalian ORC complex does not have noticeable DNA specificity unlike its yeast counterpart (DePamphilis, 2005) and it is more likely that new mechanisms have evolved in mammals to increase ORC occupancy at heterochromatin, including the ability of ORC to interact with H4K20 methylation marks.

Despite many attempts and similarly to other laboratories (Eid *et al*, 2016), we were unable to identify a specific H4K20me2 antibody for ChIP experiments, which has precluded exploring further the impact of this Suv4-20h-mediated H4K20me state in our studies. Although we cannot rule out a role of H4K20me2 in DNA replication, our results suggest that this function would be restrained to late-replicating heterochromatin regions. However, H4K20me2 is an ubiquitous histone modification found at almost 80% of histone H4 molecules (Pesavento *et al*, 2008) and it is therefore difficult to envision H4K20me2 as a specific determinant of replication origin activity in heterochromatin. Instead, Suv4-20h-mediated H4K20me3 is a hallmark of heterochromatin and our results show that this H4K20me state is particularly enriched at a subset of late-firing origins in heterochromatin domains retarded in Suv4-20h-null cells. In the absence of this mark, we showed that the licensing and firing of these origins are strongly reduced. The specific affinity of ORCA for H4K20me3 could explain why this histone methylation is required for sustaining proper replication origin activity in heterochromatin regions (Vermeulen *et al*, 2010; Beck *et al*, 2012b). Indeed, previous studies have shown that ORCA is a heterochromatin protein that facilitates the recruitment of ORC to chromatin and, in the absence of this factor, the MCM2-7 loading is impaired (Shen *et al*, 2010). In line with this, we showed that loss of H4K20me3 triggers a decrease in

ORCA binding followed by a reduction in the recruitment of MCMs at a specific subset of late-firing origins in Suv4-20h-null and $H4^{K20A}$ cells (Figs 5 and 6). Our results are also in agreement with a recent genome-wide study showing that ORCA is enriched at late-firing origins in chromatin regions associated with H3K9me3 and methyl-CpG (Wang *et al*, 2016), two repressive chromatin marks that often coincide with H4K20me3 (Benetti *et al*, 2007; Pannetier *et al*, 2008). In addition to its role in replication origin licensing, it has been proposed that ORCA could also mediate heterochromatin formation by associating with these repressive marks and regulating their deposition on chromatin through the interaction with the enzymes responsible for these marks (Giri & Prasanth, 2015). In agreement with these results, we observed a strong decrease of H4K20me3 at late-firing origins in ORCA-depleted cells (Fig 6). Since H3K9me3 appears as a prerequisite for the subsequent H4K20me3 (Schotta *et al*, 2004), we therefore propose that the initial recruitment of ORCA could depend on H3K9me3 and the subsequent appearance of H4K20me3 signal at some origins would serve to reinforce and stabilize ORCA binding to these specific sites, which in turn is pivotal to ensure an appropriate loading of pre-RC complex and proper replication timing in more condensed regions of the genome. It is also interesting to note that the decrease of H4K20me3 mark is generally associated with a negative cancer prognosis (Koturbash *et al*, 2012), suggesting that the observed alterations in heterochromatin replication upon loss of Suv4-20h and H4K20me3 could contribute to malignant transformation. Consistent with this possibility, Suv4-20h-null cells exhibit a high sensitivity to stress conditions resulting in abnormal mitotic chromosome behavior and genome instability (Schotta *et al*, 2008; Hahn *et al*, 2013), two hallmarks of pre-cancerous cells that can be the consequences of reduced origin activity and delayed late-replication domains (Donley & Thayer, 2013).

Because of the cell-cycle regulation of PR-Set7 activity, H4K20me1 is mainly synthesized during G2/M transition and converted to H4K20me2/3 afterward, leaving H4K20 largely un-methylated after replication and during most of the G2-phase (Saredi *et al*, 2016). This cell-cycle regulation is essential to prevent premature origin licensing and re-replication during S/G2-phase (Tardat *et al*, 2010), as confirmed by our results with H4K20A mutant (Fig 1). However, the reset in H4K20 methylation states after each round of DNA replication could also provide a window of opportunity for changes in the chromosomal distribution of H4K20 methylation and thus in the choice of active replication origins among several potential origins. Indeed, late-firing origins are generally cell type specific and variations in replication timing are controlled primarily at the level of origin activity and often associated with chromatin structure changes that drive cell differentiation (Smith *et al*, 2016). Determining how PR-Set7 and Suv4-20h enzymes find their specific targets on chromatin will therefore be exciting and fruitful research avenues to focus on and help to unravel the epigenetic mechanisms that regulate the usage of late-firing origins in each cell lineage.

Materials and Methods

Plasmids and shRNA constructs

pCDNA-UAS(5X)-LUC, pMSCV PR-$SET7^{FY/AA}$, and PMSCV PR-$Set7^{FY/AA\text{-}SETmut}$ were previously described (Tardat *et al*, 2010). pQCXIP $H4^{WT}$ was generated by cloning the histone H4 cDNA and a C-terminal 3× FLAG sequence as an Age1-Not1 fragment into the pQCXIP vector (Clontech). pQCXIP $H4^{K20A}$ substitution mutant was generated by site-directed mutagenesis (Agilent). pQCXIP GAL4-PRSet7 and pQCXIH 3xFlag-ORC2, ORCA, MCM2, and MCM5 were generated as described for pQCXIP $H4^{WT}$. pDEST-ZEO-$GAL4^{DBD}$-RfA plasmid was first generated by cloning $GAL4^{DBD}$ and RfA sequences into pCDNA3-ZEO and subsequently used to shuttle $PRSet7^{WT}$ and $PR\text{-}Set7^{SETmut}$ sequence from pDON221 vectors using clonase LR in order to generate pZEO-GAL4-$PR\text{-}Set7^{WT}$ and pZEO-GAL4-$PR\text{-}Set7^{SETmut}$. Control and ORCA shRNA lentiviral constructs (Sigma) were previously described (Chan & Zhang, 2012), and viral production and infection were performed as described in Tardat *et al* (2007).

Cell culture and establishment of stable cell lines

Cells were grown in Dulbecco's modified Eagle's medium (Invitrogen) with 10% fetal bovine serum (Sigma). For Suv4-20h inhibition in human cells, A-196 (Sigma) was added to a final concentration of 5 μM. Primary mouse embryonic fibroblast cells with inducible deletion of Suv4-20h1 (E364.2) were established by standard procedures from $Suv4\text{-}20h1^{flox/-}$; $Suv4\text{-}20h2^{-/-}$; Cre-ER embryos at E13.5 as described previously (Hayashi & McMahon, 2002; Schotta *et al*, 2008). As oxidative stress is associated with the loss of Suv4-20h enzymes (Schotta *et al*, 2008), $MEFs^{364.2}$ were cultured under low oxygen conditions in a tri-gas incubator containing 2% O_2 and 5% CO_2. FLAG-tagged pre-RC protein expression was established by transduction with the appropriate pQCXIP retroviral vectors. Deletion of floxed *Suv4-20h1* allele in MEF364.2 lines was achieved by treatment with 4-hydroxytamoxifen (1 μM) for 48 h. Establishment of GAL4 and GAL4-PR-Set7WT and GAL4-$PRSet7^{SETmut}$-expressing HEK293 $EBNA1^+$ cell lines were established by transfection of pZEO vectors followed by Zeocin selection (20 μg/ml).

Fluorescence-activated cell sorting (FACS) analysis

Cells were prepared as described previously (Tardat *et al*, 2010). For cell-cycle analysis, cells were washed with PBS and resuspended in PBS containing 7-amino-actinomycin D (Sigma) and RNase A (100 mg/ml) for 4 h at room temperature. Samples were run on a FACSCalibur (Becton Dickinson) and data analysis was performed using Flowjo software (Tree Star).

ChIP-qPCR

ChIP experiments with MEFs were performed as described previously (Tardat *et al*, 2010). ChIP-qPCR on EBV episomes was performed with transfected HEK293 $EBNA1^+$ cell lines. Detailed methods and primer sequences used for qPCR are available in Appendix Supplementary Methods. ChIP was performed with 300 μg of sheared chromatin with the appropriate antibody as follows: anti-GAL4 (Santa Cruz), anti-FLAG M2 (Sigma), anti-H4K20me1 (Diagenode), anti-H4K20me3 (Abcam and Diagenode), anti-ORCA (Bethyk), and anti-MCM (Ritzi *et al*, 2003). Quantitative PCR analysis was performed using the Roche LightCycler 480 System and the SYBR Green I Master (Roche) according to the

manufacturer's instructions. Quantitative PCR values were calculated as fold enrichment relative to isotype IgG control.

Nascent DNA strand purifications and analysis

Nascent strands (NS) were purified as described previously (Cayrou *et al*, 2011). Briefly, after extraction by DNAsol, NS are crudely separated from genomic DNA by sucrose gradient. Fractions of interest containing NS were then processed by the lambda exonuclease to eliminate contaminating DNA. Three samples were collected from three independent cell cultures. Control was obtained after treatment of the high sucrose fractions (which do not contain NS) by lambda exonuclease digestion, in order to remove lambda exonuclease artefactual digestion. NS levels at specific origins were then evaluated by qPCR using specific sets of primers (Appendix Table S2) with the Roche LightCycler 480 System and the SYBR Green I Master (Roche).

Immunoblot analysis and small-scale biochemical fractionation

The following antibodies were used: anti-PRSet7 (1:1,000, Cell Signaling), anti-H4 and anti-H4K20me1, me2, me3 (1:1,000, Cell Signaling), anti-H4 acetylation (Active motif, 1:1,000), anti-H3K9me3 (1:1,000, Abcam), anti-FLAG (1:1,000, Sigma), anti-H3K4me3 (1:1,000; Abcam), anti-H3K27me3 (1:2,000; Upstate), anti-GAL4^{DBD} (1:10,000, Santa Cruz), anti-MEK1 (1:1,000, Millipore), anti-HCF-1 (1:5,000), anti-ORCA (1:1,000, Bethyl), and anti-MCM (Cell Signaling). Small-scale biochemical fractionation to purify chromatin-enriched fraction was prepared with 10^7 cells as described previously (Tardat *et al*, 2010).

Plasmid replication assay

Detailed protocol is available in the Appendix Supplementary Methods. GFP-positive reporter plasmids (1 μg) were transfected into HEK293 EBNA1$^+$ cell line stably expressing the respective GAL4-fusion protein using Lipofectamine 2000 (Life technologies). Transfections with comparable efficiencies were verified by visualizing GFP-positive cells. Six days post-transfection, cells were harvested according to the HIRT protocol (Gerhardt *et al*, 2006). After centrifugation (2,000 × *g*) for 1 h at 4°C, DNA was purified by phenol–chloroform extraction and digested with 40 U *Dpn*I (NEB) in the presence of RNase (Roche). Digested DNA (300 ng) was electroporated into Electromax DH10B competent cells (Invitrogen) and ampicillin-resistant colonies, representing the number of recovered plasmids, were counted. The FR-DS plasmid was always transfected in parallel, and the number of resulting colonies was used for normalization. Statistical analysis of replication efficiency was performed using paired Student's *t*-test.

Replication-timing analysis

A detailed method is provided as Appendix Supplementary Methods. Briefly, 30×10^6 cells were incubated with BrdU for 1 h before ethanol fixation. Fixed cells were sorted into early and late S-phase fractions using INFLUX 500 (Cytopeia BD Biosciences). After lysis and anti-BrdU immunoprecipitation, whole-genome amplification was conducted (WGA, Sigma) and early and late neo-synthesized DNAs were labeled with Cy3 and Cy5 ULS molecules (Genomic DNA Labeling Kit, Agilent). The hybridization was performed according to the manufacturer's instructions on 4 × 180K mouse microarrays (SurePrint G3 Mouse CGH Microarray Kit, 4 × 180K, AGILENT Technologies, reference genome: mm9). Microarrays were scanned with an Agilent High-Resolution C Scanner using a resolution of 2 μm and the autofocus option. Feature extraction was performed with the Feature Extraction 9.1 software (Agilent technologies). Analysis was performed with the Agilent Genomic Workbench 5.0 software. The $\log_2$ ratio timing profiles were smoothed using the Agilent Genomic Workbench 5.0 software with the Triangular Moving Average option (500-kb windows). The analysis of replication-timing data was performed using algorithms from CGH applications (Agilent Genomic Workbench 5.0 software), particularly the aberration detection algorithms (*Z*-score with a threshold of 1.8) that define the boundaries and magnitudes of the regions of DNA loss or gain corresponding to the late- and early-replicating domains, respectively. A Student test (*t*-test) was performed on the average of the $\log^2$ values of every domain with R program 3.2.3 and significant difference is annotated when *P*-value $< 10^{-3}$. The intersection with different data sets was performed with GALAXY tools and *t*-test was performed to identify significant differences. The microarray data have been deposited in the Gene Expression Omnibus (GEO) (accession no. GSE69084). Positions of genes used for gene coverage come from RefSeq mm9. Positions of H3K27ac peaks used for coverage come from GSM1631248 (GEO database). Positions of H3K9me2 peaks used for coverage come from GSM887877 (GEO database).

Expanded View for this article is available online.

Acknowledgements

This work was supported by grants from Plan-Cancer 2009/2013 (C13106FS), from Ligue Nationale Contre le Cancer (RS16/75-108), Agence Nationale pour la Recherche (ANR-14-CE10-0008-02), Fondation pour la recherche Médicale, and German Research Foundation (DFG-SFB1064 TP05). Institutional Support was provided by the Institut National de la Santé et de la Recherche Médicale (INSERM), by the Centre National de la Recherche Scientifique (CNRS), and by HMGU. We thank Z. Zhang for ORCA and shRNA plasmids. F.I. and J.B. were supported by fellowships from LNCC, FRM, and Association pour la Recherche contre le Cancer.

Author contributions

JB, FI, NK, PP, CC, AFA, JCC, CG, and EJ performed experiments and analyzed data. EJ conceived the project and AS, JJC, and EJ supervised the study. GS generated reagents. CG, JD, CS, GB, and MM provided conceptual advice on study and interpretation of the data. CG, AS, J-CC, and EJ wrote the manuscript. CG, J-CC, and EJ revised the manuscript.

Conflict of interest

The authors declare that they have no conflict of interest.

References

Arias EE, Walter JC (2007) Strength in numbers: preventing rereplication via multiple mechanisms in eukaryotic cells. *Genes Dev* 21: 497 – 518

Beck DB, Burton A, Oda H, Ziegler-Birling C, Torres-Padilla M-E, Reinberg D (2012b) The role of PR-Set7 in replication licensing depends on Suv4-20h. *Genes Dev* 26: 2580 – 2589

Beck DB, Oda H, Shen SS, Reinberg D (2012a) PR-Set7 and H4K20me1: at the crossroads of genome integrity, cell cycle, chromosome condensation, and transcription. *Genes Dev* 26: 325 – 337

Bell SD, Botchan MR (2013) The minichromosome maintenance replicative helicase. *Cold Spring Harb Perspect Biol* 5: a012807

Benetti R, Gonzalo S, Jaco I, Schotta G, Klatt P, Jenuwein T, Blasco MA (2007) Suv4-20h deficiency results in telomere elongation and derepression of telomere recombination. *J Cell Biol* 178: 925 – 936

Besnard E, Babled A, Lapasset L, Milhavet O, Parrinello H, Dantec C, Marin J-M, Lemaitre J-M (2012) Unraveling cell type-specific and reprogrammable human replication origin signatures associated with G-quadruplex consensus motifs. *Nat Struct Mol Biol* 19: 837 – 844

Blow JJ, Ge XQ, Jackson DA (2011) How dormant origins promote complete genome replication. *Trends Biochem Sci* 36: 405 – 414

Bowers JL, Randell JCW, Chen S, Bell SP (2004) ATP hydrolysis by ORC catalyzes reiterative Mcm2-7 assembly at a defined origin of replication. *Mol Cell* 16: 967 – 978

Brustel J, Tardat M, Kirsh O, Grimaud C, Julien E (2011) Coupling mitosis to DNA replication: the emerging role of the histone H4-lysine 20 methyltransferase PR-Set7. *Trends Cell Biol* 21: 452 – 460

Cayrou C, Coulombe P, Vigneron A, Stanojcic S, Ganier O, Peiffer I, Rivals E, Puy A, Laurent-Chabalier S, Desprat R, Méchali M (2011) Genome-scale analysis of metazoan replication origins reveals their organization in specific but flexible sites defined by conserved features. *Genome Res* 21: 1438 – 1449

Cayrou C, Ballester B, Peiffer I, Fenouil R, Coulombe P, Andrau J-C, van Helden J, Méchali M (2015) The chromatin environment shapes DNA replication origin organization and defines origin classes. *Genome Res* 25: 1873 – 1885

Chan KM, Zhang Z (2012) Leucine-rich repeat and WD repeat-containing protein 1 is recruited to pericentric heterochromatin by trimethylated lysine 9 of histone H3 and maintains heterochromatin silencing. *J Biol Chem* 287: 15024 – 15033

Comoglio F, Schlumpf T, Schmid V, Rohs R, Beisel C, Paro R (2015) High-resolution profiling of *Drosophila* replication start sites reveals a DNA shape and chromatin signature of metazoan origins. *Cell Rep* 11: 821 – 834

Das SP, Borrman T, Liu VWT, Yang SC-H, Bechhoefer J, Rhind N (2015) Replication timing is regulated by the number of MCMs loaded at origins. *Genome Res* 25: 1886 – 1892

DePamphilis ML (2005) Cell cycle dependent regulation of the origin recognition complex. *Cell Cycle Georget Tex* 4: 70 – 79

Ding Q, MacAlpine DM (2011) Defining the replication program through the chromatin landscape. *Crit Rev Biochem Mol Biol* 46: 165 – 179

Donley N, Thayer MJ (2013) DNA replication timing, genome stability and cancer: late and/or delayed DNA replication timing is associated with increased genomic instability. *Semin Cancer Biol* 23: 80 – 89

Eid A, Rodriguez-Terrones D, Burton A, Torres-Padilla M-E (2016) SUV4-20 activity in the preimplantation mouse embryo controls timely replication. *Genes Dev* 30: 2513 – 2526

Fragkos M, Ganier O, Coulombe P, Méchali M (2015) DNA replication origin activation in space and time. *Nat Rev Mol Cell Biol* 16: 360 – 374

Gerhardt J, Jafar S, Spindler M-P, Ott E, Schepers A (2006) Identification of new human origins of DNA replication by an origin-trapping assay. *Mol Cell Biol* 26: 7731 – 7746

Giri S, Prasanth SG (2015) Association of ORCA/LRWD1 with repressive histone methyl transferases mediates heterochromatin organization. *Nucl Austin Tex* 6: 435 – 441

Hahn M, Dambacher S, Dulev S, Kuznetsova AY, Eck S, Wörz S, Sadic D, Schulte M, Mallm J-P, Maiser A, Debs P, von Melchner H, Leonhardt H, Schermelleh L, Rohr K, Rippe K, Storchova Z, Schotta G (2013) Suv4-20h2 mediates chromatin compaction and is important for cohesin recruitment to heterochromatin. *Genes Dev* 27: 859 – 872

Hammerschmidt W, Sugden B (2013) Replication of Epstein-Barr viral DNA. *Cold Spring Harb Perspect Biol* 5: a013029

Hayashi S, McMahon AP (2002) Efficient recombination in diverse tissues by a tamoxifen-inducible form of Cre: a tool for temporally regulated gene activation/inactivation in the mouse. *Dev Biol* 244: 305 – 318

Hoggard T, Shor E, Müller CA, Nieduszynski CA, Fox CA (2013) A Link between ORC-origin binding mechanisms and origin activation time revealed in budding yeast. *PLoS Genet* 9: e1003798

Jørgensen S, Elvers I, Trelle MB, Menzel T, Eskildsen M, Jensen ON, Helleday T, Helin K, Sørensen CS (2007) The histone methyltransferase SET8 is required for S-phase progression. *J Cell Biol* 179: 1337 – 1345

Jørgensen S, Schotta G, Sørensen CS (2013) Histone H4 lysine 20 methylation: key player in epigenetic regulation of genomic integrity. *Nucleic Acids Res* 41: 2797 – 2806

Koturbash I, Simpson NE, Beland FA, Pogribny IP (2012) Alterations in histone H4 lysine 20 methylation: implications for cancer detection and prevention. *Antioxid Redox Signal* 17: 365 – 374

Kuo AJ, Song J, Cheung P, Ishibe-Murakami S, Yamazoe S, Chen JK, Patel DJ, Gozani O (2012) The BAH domain of ORC1 links H4K20me2 to DNA replication licensing and Meier-Gorlin syndrome. *Nature* 484: 115 – 119

Leonard AC, Méchali M (2013) DNA replication origins. *Cold Spring Harb Perspect Biol* 5: a010116

Li Y, Armstrong RL, Duronio RJ, MacAlpine DM (2016) Methylation of histone H4 lysine 20 by PR-Set7 ensures the integrity of late replicating sequence domains in *Drosophila*. *Nucleic Acids Res* 44: 7204 – 7218

Liu J, Zimmer K, Rusch DB, Paranjape N, Podicheti R, Tang H, Calvi BR (2015) DNA sequence templates adjacent nucleosome and ORC sites at gene amplification origins in *Drosophila*. *Nucleic Acids Res* 43: 8746 – 8761

Lombraña R, Almeida R, Revuelta I, Madeira S, Herranz G, Saiz N, Bastolla U, Gómez M (2013) High-resolution analysis of DNA synthesis start sites and nucleosome architecture at efficient mammalian replication origins. *EMBO J* 32: 2631 – 2644

McGuffee SR, Smith DJ, Whitehouse I (2013) Quantitative, genome-wide analysis of eukaryotic replication initiation and termination. *Mol Cell* 50: 123 – 135

McKay DJ, Klusza S, Penke TJR, Meers MP, Curry KP, McDaniel SL, Malek PY, Cooper SW, Tatomer DC, Lieb JD, Strahl BD, Duronio RJ, Matera AG (2015) Interrogating the function of metazoan histones using engineered gene clusters. *Dev Cell* 32: 373 – 386

Méchali M, Yoshida K, Coulombe P, Pasero P (2013) Genetic and epigenetic determinants of DNA replication origins, position and activation. *Curr Opin Genet Dev* 23: 124 – 131

Oda H, Hübner MR, Beck DB, Vermeulen M, Hurwitz J, Spector DL, Reinberg D (2010) Regulation of the histone H4 monomethylase PR-Set7 by CRL4 (Cdt2)-mediated PCNA-dependent degradation during DNA damage. *Mol Cell* 40: 364 – 376

Palacios DeBeer MA, Muller U, Fox CA (2003) Differential DNA affinity specifies roles for the origin recognition complex in budding yeast heterochromatin. *Genes Dev* 17: 1817 – 1822

Pannetier M, Julien E, Schotta G, Tardat M, Sardet C, Jenuwein T, Feil R (2008) PR-SET7 and SUV4-20H regulate H4 lysine-20 methylation at imprinting control regions in the mouse. *EMBO Rep* 9: 998 – 1005

Pesavento JJ, Yang H, Kelleher NL, Mizzen CA (2008) Certain and progressive methylation of histone H4 at lysine 20 during the cell cycle. *Mol Cell Biol* 28: 468 – 486

Picard F, Cadoret J-C, Audit B, Arneodo A, Alberti A, Battail C, Duret L, Prioleau M-N (2014) The spatiotemporal program of DNA replication is associated with specific combinations of chromatin marks in human cells. *PLoS Genet* 10: e1004282

Pope BD, Gilbert DM (2013) The replication domain model: regulating replicon firing in the context of large-scale chromosome architecture. *J Mol Biol* 425: 4690 – 4695

Pope BD, Ryba T, Dileep V, Yue F, Wu W, Denas O, Vera DL, Wang Y, Hansen RS, Canfield TK, Thurman RE, Cheng Y, Gülsoy G, Dennis JH, Snyder MP, Stamatoyannopoulos JA, Taylor J, Hardison RC, Kahveci T, Ren B *et al* (2014) Topologically associating domains are stable units of replication-timing regulation. *Nature* 515: 402 – 405

Prioleau M-N, MacAlpine DM (2016) DNA replication origins-where do we begin? *Genes Dev* 30: 1683 – 1697

Remus D, Diffley JFX (2009) Eukaryotic DNA replication control: lock and load, then fire. *Curr Opin Cell Biol* 21: 771 – 777

Renard-Guillet C, Kanoh Y, Shirahige K, Masai H (2014) Temporal and spatial regulation of eukaryotic DNA replication: from regulated initiation to genome-scale timing program. *Semin Cell Dev Biol* 30: 110 – 120

Rhind N, Gilbert DM (2013) DNA replication timing. *Cold Spring Harb Perspect Med* 5: a010132

Ritzi M, Tillack K, Gerhardt J, Ott E, Humme S, Kremmer E, Hammerschmidt W, Schepers A (2003) Complex protein-DNA dynamics at the latent origin of DNA replication of Epstein-Barr virus. *J Cell Sci* 116: 3971 – 3984

Sakaguchi A, Karachentsev D, Seth-Pasricha M, Druzhinina M, Steward R (2008) Functional characterization of the *Drosophila* Hmt4-20/Suv4-20 histone methyltransferase. *Genetics* 179: 317 – 322

Saredi G, Huang H, Hammond CM, Alabert C, Bekker-Jensen S, Forne I, Reverón-Gómez N, Foster BM, Mlejnkova L, Bartke T, Cejka P, Mailand N, Imhof A, Patel DJ, Gorth A (2016) H4K20me0 marks post-replicative chromatin and recruits the TONSL–MMS22L DNA repair complex. *Nature* 534: 714 – 718

Schotta G, Lachner M, Sarma K, Ebert A, Sengupta R, Reuter G, Reinberg D, Jenuwein T (2004) A silencing pathway to induce H3-K9 and H4-K20 trimethylation at constitutive heterochromatin. *Genes Dev* 18: 1251 – 1262

Schotta G, Sengupta R, Kubicek S, Malin S, Kauer M, Callén E, Celeste A, Pagani M, Opravil S, De La Rosa-Velazquez IA, Espejo A, Bedford MT, Nussenzweig A, Busslinger M, Jenuwein T (2008) A chromatin-wide transition to H4K20 monomethylation impairs genome integrity and programmed DNA rearrangements in the mouse. *Genes Dev* 22: 2048 – 2061

Shen Z, Sathyan KM, Geng Y, Zheng R, Chakraborty A, Freeman B, Wang F, Prasanth KV, Prasanth SG (2010) A WD-repeat protein stabilizes ORC binding to chromatin. *Mol Cell* 40: 99 – 111

Siddiqui K, On KF, Diffley JFX (2013) Regulating DNA replication in eukarya. *Cold Spring Harb Perspect Biol* 5: a012930

Smith OK, Aladjem MI (2014) Chromatin structure and replication origins: determinants of chromosome replication and nuclear organisation. *J Mol Biol* 426: 3330 – 3341

Smith OK, Kim R, Fu H, Martin MM, Lin CM, Utani K, Zhang Y, Marks AB, Lalande M, Chamberlain S, Libbrecht MW, Bouhassira EE, Ryan MC, Noble WS, Aladjam MI (2016) Distinct epigenetic features of differentiation-regulated replication origins. *Epigenetics Chromatin* 9: 18

Takawa M, Cho HS, Hayami S, Toyokawa G, Kogure M, Yamane Y, Iwai Y, Maejima K, Ueda K, Masuda A, Dohmae N, Field HI, Tsunoda T, Kobayashi T, Akasu T, Sugiyama M, Ohnuma S, Atomi Y, Ponder BA, Nakamura Y *et al* (2012) Histone lysine methyltransferase SETD8 promotes carcinogenesis by deregulating PCNA expression. *Cancer Res* 72: 3217 – 3227

Tardat M, Murr R, Herceg Z, Sardet C, Julien E (2007) PR-Set7-dependent lysine methylation ensures genome replication and stability through S phase. *J Cell Biol* 179: 1413 – 1426

Tardat M, Brustel J, Kirsh O, Lefevbre C, Callanan M, Sardet C, Julien E (2010) The histone H4 Lys 20 methyltransferase PR-Set7 regulates replication origins in mammalian cells. *Nat Cell Biol* 12: 1086 – 1093

Valton A-L, Hassan-Zadeh V, Lema I, Boggetto N, Alberti P, Saintomé C, Riou J-F, Prioleau M-N (2014) G4 motifs affect origin positioning and efficiency in two vertebrate replicators. *EMBO J* 33: 732 – 746

Vermeulen M, Eberl HC, Matarese F, Marks H, Denissov S, Butter F, Lee KK, Olsen JV, Hyman AA, Stunnenberg HG, Mann M (2010) Quantitative interaction proteomics and genome-wide profiling of epigenetic histone marks and their readers. *Cell* 142: 967 – 980

Wang Y, Khan A, Marks AB, Smith OK, Giri S, Lin Y-C, Creager R, MacAlpine DM, Prasanth KV, Aladjem MI, Prasanth SG (2016) Temporal association of ORCA/LRWD1 to late-firing origins during G1 dictates heterochromatin replication and organization. *Nucleic Acids Res* 45: 2490 – 2502